Title

Mechanisms of transmission ratio distortion at hybrid sterility loci within and between *Mimulus* species

Authors

Rachel E. Kerwin[1], Andrea L. Sweigart[1,*]

Author affiliations

[1] Department of Genetics, University of Georgia, Athens, GA 30602

*Corresponding author; email: sweigart@uga.edu; phone: (706)-542-7001

ABSTRACT

Hybrid incompatibilities are a common correlate of genomic divergence and a potentially important contributor to reproductive isolation. However, we do not yet have a detailed understanding of how hybrid incompatibility loci function and evolve within their native species, or why they are dysfunctional in hybrids. Here, we explore these issues for a well-studied, two-locus hybrid incompatibility between *hybrid male sterility 1* (*hms1*) and *hybrid male sterility 2* (*hms2*) in the closely related yellow monkeyflower species *Mimulus guttatus* and *M. nasutus*. By performing reciprocal backcrosses with introgression lines, we find evidence for gametic expression of the *hms1-hms2* incompatibility. Surprisingly, however, hybrid transmission ratios at *hms1* do not reflect this incompatibility, suggesting additional mechanisms counteract the effects of gametic sterility. Indeed, our backcross experiment shows hybrid transmission bias toward *M. guttatus* through both pollen and ovules, an effect that is particularly strong when *hms2* is homozygous for *M. nasutus* alleles. In contrast, we find little evidence for *hms1* transmission bias in crosses within *M. guttatus*, providing no indication of selfish evolution at this locus. Although we do not yet have sufficient genetic resolution to determine if hybrid sterility and transmission ratio distortion map to the same loci, our preliminary fine-mapping uncovers a genetically independent hybrid lethality system involving at least two loci linked to *hms1*. This fine-scale dissection of transmission ratio distortion at *hms1* and *hms2* provides insight into genomic differentiation between closely related *Mimulus* species and reveals multiple mechanisms of hybrid dysfunction.

INTRODUCTION

Hybrid incompatibilities are a common outcome of genomic divergence among closely related species. Across diverse taxa, a number of genes for hybrid inviability and sterility have been identified (see Presgraves 2010; Maheshwari and Barbash 2011; Sweigart and Willis 2012; Ouyang and Zhang 2013), but we still know very little about how such genes function and initially evolve within their native species. One possibility is that the initial mutations are selectively neutral and become fixed by random genetic drift. Alternatively, the mutations might increase in frequency because they benefit the native species for reasons that are incidental to their role in reproductive isolation – by promoting ecological adaptation, for example (Schluter and Conte 2009). Yet another possibility is that hybrid incompatibilities arise through recurrent bouts of intragenomic conflict within species (Frank 1991; Hurst and Pomiankowski 1991). In this last scenario, selfish genetic elements (*e.g.*, transposons, meiotic drivers, gamete killers) manipulate host reproduction to bias their own transmission. Because these actions are often detrimental to host fitness, there is then selective pressure for compensatory mutations or suppressors to neutralize the effects of selfish evolution (Burt and Trivers 2006).

The idea that intragenomic conflict involving segregation distorters might be a major source of hybrid incompatibilities has resurged in recent years (Johnson 2010; McDermott and Noor 2010; Presgraves 2010; Crespi and Nosil 2013), largely due to influential studies in *Drosophila* that have mapped hybrid segregation distortion and hybrid sterility to the same genomic locations (Tao et al. 2001; Phadnis and Orr 2009b; Zhang et al. 2015). In plants, too, classic and recent crossing studies have revealed "gamete killers" that affect both transmission ratios and fertility; at these loci, one parental allele causes the abortion of gametes carrying the other allele (*e.g.*, tobacco: (Cameron and Moav 1957), wheat: (Loegering and Sears 1963), tomato: (Rick 1966), rice: (Sano 1990; Long et al. 2008; Yang et al. 2012), Arabidopsis: (Simon et al. 2016)). Although suggestive of a causal link between selfish genetic elements and hybrid incompatibilities, few studies have proven a history of segregation distortion *within* species. Thus, in most cases, an alternative possibility is that segregation distortion acts

exclusively in hybrid genetic backgrounds, and is a consequence rather than a cause of the incompatibility.

In seed plants, hybrid incompatibilities can act in either the diploid sporophyte or the haploid gametophyte, two stages of the life cycle that are controlled by different sets of genes and subject to distinct evolutionary forces (Walbot and Evans 2003; Gossmann et al. 2014; Gossmann et al. 2016). Unlike in animal systems, which have very little haploid gene expression in sperm or egg cells (Braun et al. 1989; Barreau et al. 2008), thousands of genes are expressed in plant gametophytes (*i.e.*, pollen and embryo sacs in angiosperms) (Wuest et al. 2010; Rutley and Twell 2015). As a result, hybrid sterility in plants can be caused by genetic incompatibilities that affect the haploid gametophytes or the diploid sporophytic tissues surrounding the gametes (*e.g.*, tapetum for pollen, ovule cells for the embryo sac). Of these two possibilities, the former appears to be much more common among the ~50 hybrid sterility loci that have been identified between subspecies of Asian cultivated rice, *Oryza sativa ssp. japonica* and *O. sativa ssp. indica* (Morishima et al. 1991; Ouyang and Zhang 2013). A large number of gametic incompatibilities have also been shown to contribute to transmission ratio distortion in crosses between populations of *Arabidopsis lyrata* (Leppala et al. 2013). This bias toward gametic incompatibilities might be due to differences in the number of mutations that affect the two classes of hybrid sterility and/or to the fact that recessive alleles are exposed in the haploid gametophyte (similar to genes on heteromorphic sex chromosomes). Additionally, rates of evolution might be accelerated for gametophytic genes due to sex-specific selection (Gossmann et al. 2014). It is also possible that intragenomic conflict is more common in the gametophyte; any selfish genetic element that can disable gametes carrying the alternative allele will have a direct impact on its own transmission.

Of the handful of plant hybrid sterility genes that have been cloned, all are in rice, most are gametic, and many appear to have evolved via neutral processes. The two most straightforward examples involve pollen defects caused by loss-of-function alleles at duplicate genes (Mizuta et al. 2010; Yamagata et al. 2010), consistent with a model of divergent resolution via degenerative mutations and genetic drift (Werth and Windham 1991; Lynch and Force 2000). The remaining six cases all involve gamete killers (Long et al. 2008; Kubo et al. 2011; Yang et al. 2012; Kubo et al. 2016a; Kubo et al. 2016b; Yu

et al. 2016), which might be taken as evidence for pervasive selfish evolution within rice species. However, molecular characterization of these hybrid sterility systems has provided little support for this scenario. For example, the *S5* locus causes female sterility in *japonica-indica* hybrids when gametes carry an incompatible combination of "killer" and "protector" alleles at three, tightly linked genes (Yang et al. 2012). The two domesticated subspecies carry null alleles in distinct components of the killer-protector system. Because both derived haplotypes are perfectly compatible with the ancestral haplotype, it seems unlikely that they entailed fitness costs. Although it is conceivable that intragenomic conflict played a role in the initial formation of the *S5* haplotype (*i.e.*, the ancestral killer/protector combination might represent a resolved conflict), it does not seem to be the cause of the current reproductive barrier between *japonica* and *indica*. Similarly, at the *Sa* locus, which causes *japonica-indica* hybrid male sterility, patterns of molecular variation and the prevalence of "neutral" alleles that are compatible in all crosses suggest that hybrid dysfunction may have evolved unopposed by natural selection (Long et al. 2008; Sweigart and Willis 2012). A key feature of these gamete killers is that they are caused by two or more tightly linked, epistatic genes (Long et al. 2008; Yang et al. 2012; Kubo 2013; Kubo et al. 2016a). Adding to the complexity, some of them require additional, unlinked loci that act sporophytically (Kubo et al. 2011; Kubo et al. 2016a; Kubo et al. 2016b). Taken together, these studies suggest that hybrid sterility in rice is polygenic and might evolve without significant fitness costs within species. However, it is not yet clear if these themes are generalizable to other plant systems.

Here we investigate patterns of transmission ratio distortion associated with a two-locus hybrid sterility system between the closely related monkeyflower species, *Mimulus guttatus* and *M. nasutus*. Previously, we fine-mapped the two incompatibility loci – *hybrid male sterility 1* (*hms1*) and *hybrid male sterility 2* (*hms2*) – to small nuclear genomic regions of ~60 kb each on chromosomes 6 and 13 (Sweigart and Flagel 2015). We also discovered evidence that the *hms1* incompatibility allele is involved in a partial selective sweep within a single population of *M. guttatus*, but the underlying cause of the sweep is unknown (Sweigart and Flagel 2015). Additionally, because the *hms1* sterility allele is embedded in a nearly invariant, 320-kb haplotype, it is not yet clear whether *hms1* or a linked locus is the target of the sweep. This polymorphic hybrid sterility

system provides a unique opportunity to test directly whether selfish evolution within species can lead to incompatibilities between species.

Previously, in crosses between *M. guttatus* and *M. nasutus*, we observed transmission ratio distortion (TRD) of genotypes at both *hms1* and *hms2* (Sweigart et al. 2006; Sweigart and Flagel 2015), but the causes have remained unexplored. Additionally, these previous studies did not test directly whether the *hms1-hms2* incompatibility acts in the gametophyte or sporophyte, although patterns of F_2 hybrid sterility seemed to suggest the latter. Results from these studies suggested that the incompatibility acts in the diploid sporophyte with the *M. guttatus* allele at *hms1* acting dominantly in combination with recessive *M. nasutus* alleles at *hms2* to cause nearly complete male sterility and partial female sterility (Sweigart et al. 2006). Consistent with this genetic model, pollen viability is ~20% in F_2 hybrids that are heterozygous for *hms1* and homozygous for *M. nasutus* alleles at *hms2* ($hms1_{GN}$; $hms2_{NN}$), much lower than the 50% expected for a strictly gametic hybrid incompatibility (with $hms1_G$; $hms2_N$ causing dysfunction). Moreover, because a gametic hybrid incompatibility should cause transmission bias at *both* interacting loci, we would expect a deficit of *M. guttatus* alleles at *hms1* equal to that of *M. nasutus* alleles at *hms2*. Although F_2 hybrids do indeed show a deficit of *M. nasutus* alleles at *hms2*, allelic transmission at *hms1* follows the Mendelian expectation (Sweigart et al. 2006).

In the current study, we used introgression lines (ILs) and a reciprocal backcross design to distinguish among at least four possibilities for TRD in genomic regions linked to *hms1* and *hms2:* 1) distortion through male gametes due to pollen competition and/or pollen sterility, 2) distortion through female gametes due to female meiotic drive (*e.g.*, (Fishman and Saunders 2008) and/or ovule sterility, 3) TRD through both male and female gametes due to an incompatibility that affects both gametophytes (*e.g.*, (Kubo et al. 2016a), and 4) distortion caused by selection against zygotes. In a series of crossing experiments, we investigated the mechanism of TRD at *hms1* and *hms2* and addressed the following specific questions. Is hybrid transmission bias at *hms1* and/or *hms2* a simple byproduct of gametic hybrid sterility? Is there evidence for hybrid transmission bias at these loci independent of gamete sterility? Are hybrid sterility and TRD genetically separable? Does TRD at *hms1* occur within *M. guttatus*? Our results provide insight into

158 the mechanisms of hybrid sterility and transmission distortion, and into the evolutionary
159 dynamics of incompatibility alleles within species.
160
161
162 **METHODS**
163
164 **Study system and plant lines**
165 The *Mimulus guttatus* species complex is a group of phenotypically diverse wildflowers
166 with abundant natural populations throughout much of western North America. In this
167 study, we focus on *M. guttatus* and *M. nasutus*, two members of the complex that
168 diverged roughly 200,000 years ago (Brandvain et al. 2014). These species occupy a
169 partially overlapping range, and are primarily differentiated by mating system. *M.*
170 *guttatus* is predominantly outcrossing with showy, insect-pollinated flowers, whereas *M.*
171 *nasutus* is highly self-fertilizing with reduced flowers. In geographic regions where the
172 two species co-occur, they are partially reproductively isolated by differences in floral
173 morphology, flowering phenology, and pollen-pistil interactions (Diaz and Macnair 1999;
174 Martin and Willis 2007; Fishman et al. 2014). Hybrid incompatibilities are also common,
175 but variable (Vickery 1978; Christie and Macnair 1987; Sweigart et al. 2007; Case and
176 Willis 2008; Martin and Willis 2010). Despite these barriers to interspecific gene flow,
177 sympatric populations display evidence of genome-wide introgression (Sweigart and
178 Willis 2003; Brandvain et al. 2014; Kenney and Sweigart 2016).
179 Previous work identified two nuclear incompatibility loci – *hybrid male sterility 1*
180 (*hms1*) and *hybrid male sterility 2* (*hms2*) – that cause nearly complete male sterility and
181 partial female sterility in a fraction of F_2 hybrids between an inbred line of *M. guttatus*
182 from Iron Mountain, Oregon (IM62), and a naturally inbred *M. nasutus* line from
183 Sherar's Falls, Oregon (SF5) (Sweigart et al. 2006). In 2015, Sweigart and Flagel
184 generated a large SF5-IM62 F_2 mapping population (N = 5487) to fine map *hms1* and
185 *hms2* to regions of ~60 kb on chromosome 6 and chromosome 13, respectively. Hybrids
186 carrying at least one incompatible *M. guttatus* allele at *hms1* in combination with two
187 incompatible *M. nasutus* alleles at *hms2* display extreme male sterility and partial female
188 sterility (Sweigart et al. 2006). Furthermore, the *hms1* locus is polymorphic within the

Iron Mountain population (Sweigart et al. 2007) and several inbred lines derived from that site are known to carry "compatible" alleles that do not cause hybrid sterility when crossed to *M. nasutus* (Sweigart and Flagel 2015). In experimental crosses to test for TRD at *hms1* within *M. guttatus*, we used a compatible line called IM767. In total, three inbred lines were used in different crossing schemes to test for TRD within and between species (see below). SF5 is compatible at *hms1* and incompatible at *hms2,* IM62 is incompatible at *hms1* and compatible at *hms2*, and IM767 is compatible at *hms1* and *hms2*.

All plants were grown in the greenhouse at the University of Georgia. For all crosses, seeds were planted into 96-cell flats containing Fafard 3B potting mix (Sun Gro Horticulture, Agawam, MA), stratified for 7 days at 4°C, and then placed in a greenhouse with supplemental lights set to 16-hr days. Plants were bottom-watered daily and temperatures were maintained at 24°C during the day and 16°C at night.

Introgression line (IL) crossing design to investigate mechanisms of transmission ratio distortion between *M. guttatus* and *M. nasutus*

Previously, two reciprocal nearly isogenic line (NIL) populations carrying *M. nasutus* (SF5) or *M. guttatus* (IM62) introgressions in the opposite genetic background were generated (Fishman and Willis 2005). Briefly, a single SF5 x IM62 F_1 and IM62 x SF5 F_1 individual each served as the initial seed parent then underwent four generations of backcrossing to create a BN_4 NIL population (SF5 x IM62 F_1, *M. nasutus* recurrent parent) and BG_4 NIL population (IM62 x SF5 F_1, *M. guttatus* recurrent parent). Within the BN_4 and BG_4 populations, each NIL carries a unique complement of heterozygous introgressions in a genome that is expected to be 96.875% homozygous for the recurrent parent's alleles. To determine the genomic locations of the heterozygous introgressed regions, the NILs were genotyped at microsatellite and gene-based markers distributed throughout the genome (L. Fishman, unpublished). We selected three NILs with introgressions spanning *hms1* or *hms2* for further genetic analyses. Against a largely *M. guttatus* background, the BG_4.476 NIL is heterozygous for an introgression that includes *hms1* and ~78% of the physical distance along chromosome 6. The BG_4.149 line is heterozygous for an introgression that spans ~71% of chromosome 13 and includes *hms2*.

Against a *M. nasutus* background, the $BN_4.62$ line is heterozygous for ~75% of chromosome 13, including *hms2*. In addition to these NILs, we used an *hms1* introgression line, RSB_4, created after four generations of recurrent selection for hybrid sterility with backcrossing to *M. nasutus,* starting from a sterile SF5-IM62 BC_1 individual (Sweigart et al. 2006); the heterozygous introgression spans ~50% of chromosome 6.

To characterize TRD between *M. guttatus* and *M. nasutus*, we used a multi-step crossing scheme, starting with the NILs and RSB_4 (described above), to create a set of lines carrying specific two-locus genotypes at *hms1* and *hms2*. First, to generate introgression lines (ILs) that carry heterozygous alleles at both *hms1* and *hms2* in an otherwise *M. guttatus* or *M. nasutus* genetic background, we crossed $BG_4.476$ to $BG_4.149$, and $BN_4.62$ to RSB_4. From those progeny, we identified *hms1-hms2* double heterozygotes by genotyping markers that flank *hms1* (M8 and M24) and *hms2* (M51 and MgSTS193), as described previously (Sweigart and Flagel 2015). Next, to generate individuals that carry various two-locus combinations at *hms1* and *hms2*, we self-fertilized doubly heterozygous ILs from each genetic background (*i.e.*, IL-G and IL-N = *M. guttatus* and *M. nasutus* backgrounds, respectively). These crosses are expected to yield nine different two-locus genotypes each (typical of an F_2), five of which are heterozygous at *hms1* and/or *hms2* (Figure 1). Surprisingly, one of the relevant IL-N *hms1-hms2* genotypes was not recovered ($hms1_{GG}$; $hms2_{GN}$, see Figure 1); the *hms1*-introgression could not be made homozygous for *M. guttatus* alleles against an *M. nasutus* genetic background (see Results). We assessed male fertility (*i.e.*, pollen viability) for the nine experimental IL genotypes (five for IL-G and four for IL-N) as described previously (Sweigart et al. 2006; Sweigart et al. 2007).

To test the effect of *hms1* genotype on transmission at *hms2* and vice versa, we reciprocally backcrossed each of the nine ILs to both *M. guttatus* (IM62) and *M. nasutus* (SF5) (Figure 1). Thus, for each IL, we generated four reciprocal backcross populations allowing us to dissect gender-specific transmission ratio distortion. For each IL, two of the backcrosses used the emasculated IL as the seed parent in crosses to IM62 and SF5 lines (i.e., IL-IM62 and IL-SF5) and two used the IL as the pollen parent in crosses to emasculated IM62 and SF5 plants (i.e., IM62-IL, and SF-IL). If *hms* distortion occurs through pollen (due to pollen competition or a gametic incompatibility), we expect TRD

in one or both of the backcrosses using the IL as the paternal parent, but not as the maternal parent. If, instead, female meiotic drive and/or a female gametic incompatibility occurs at these *hms* loci, we would expect to see TRD in both backcrosses with the IL as the seed parent, but not with the IL as the pollen parent. Finally, if TRD is caused by the loss of diploid zygotes (or seedlings), it should be apparent in *both* reciprocal crosses to the same recurrent parent (*i.e.*, regardless of the gender of the IL). For all crosses, the female parent was emasculated 1-2 days before hand-pollination to prevent self-pollination. Sample sizes for the progeny classes ranged from 33 to 215 individuals (average $N = 136$).

For each *hms* locus, we performed factorial ANOVAs in Jmp Pro 13.0 to examine if genotype ratios were affected by four factors: 1) IL genetic background, 2) IL genotype at the interacting *hms* locus, 3) backcross direction, and 4) identity of the recurrent parent.

Crossing design to examine transmission ratio distortion within *M. guttatus*

To determine whether transmission ratio distortion at the polymorphic *hms1* incompatibility locus occurs between incompatible and compatible alleles from the Iron Mountain population of *M. guttatus*, we generated reciprocal F_2 and backcrossed populations with IM62 and IM767. We previously determined that the IM767 inbred line carries a compatible allele at *hms1* (*i.e.*, one that does not carry the 320-kb haplotype or cause sterility in combination with SF5 alleles at *hms2*). The IM62 and IM767 inbred lines were intercrossed reciprocally and a single F_1 hybrid from each was self-fertilized to form reciprocal F_2 populations (IM62 x IM767: $N = 267$; IM767 x IM62: $N = 315$). To identify putative female- and male-specific sources of TRD, and to distinguish between meiotic/gametic mechanisms versus zygotic selection, we generated reciprocal backcrosses with IM62 and IM767. We used a single F_1 hybrid (IM62 x 767; maternal parent listed first) to generate four backcross populations to the recurrent parents (F_1-IM62 BC_1, IM62-F_1 BC_1, F_1-IM767 BC_1, IM767-F_1 BC_1). Two of these backcrosses used the emasculated F_1 as the seed parent and two used the F_1 as the pollen donor in crosses to the emasculated recurrent parents.

We also wanted to examine the effect of *M. nasutus hms2* alleles on patterns of within-*M. guttatus* TRD at *hms1*. We wondered if having *M. nasutus* alleles at *hms2* has the potential to unleash severe distortion at *hms1*, even in an otherwise *M. guttatus* genetic background. To address this question, we intercrossed IM767 with a BG_4-NIL (BG_4.275) that is heterozygous for an SF5 introgression spanning ~36% of chromosome 13 including *hms2* (in an IM62 genetic background; Figure S2). We self-fertilized two of the resulting F_1s to generate F_2 hybrids segregating for SF5 alleles at *hms2* against an IM62-IM767 F_2-like genetic background. We then genotyped at *hms*-linked markers (M183 for *hms1* and MgSTS193 for *hms2*) to identify IM62-IM767 *hms1* heterozygotes in combination with three different *hms2* genotypes: 1) IM62 homozygotes, 2) IM767 homozygotes, or 3) SF5 homozygotes. Using each of these three genotypic classes, we performed reciprocal backcrosses to IM767 (Figure S2).

Assessment of transmission ratio distortion

To examine patterns of TRD at the *hms1* and *hms2* loci, we collected leaf tissue from individual plants and isolated genomic DNA using a rapid extraction protocol (Cheung *et al*. 1993) modified for 96-well format. To infer the *hms1* and *hms2* genotypes of hybrid progeny generated from crosses between IM62 and SF5, we determined genotypes at a multiplexed set of fluorescently labeled markers that flank *hms1* (M8 and M24) and *hms2* (MgSTS193 and M51) following amplification protocols used previously (Sweigart et al. 2006; Sweigart et al. 2007). We excluded individuals with crossovers between either pair of flanking markers; based on expected frequency of double crossovers between flanking markers, genotyping error rates for *hms1* and *hms2* were each < 1%. For experimental crosses involving IM62 and IM767, only one tightly linked marker was used to infer genotype at *hms1* (M183). Based on expected crossovers between *hms1* and M183, the genotyping error rate was < 1%. All fluorescently labeled marker products were run on an ABI 3730 at the University of Georgia Genomics Facility. Genotypes were scored automatically using GeneMarker (SoftGenetics), with additional hand scoring when necessary. We used chi-square tests with two degrees of freedom to determine if *hms*-linked genotypes were significantly distorted.

RESULTS

Transmission ratio distortion in *M. nasutus-M. guttatus* F_2 hybrids

As part of previous efforts to fine-map *Mimulus* hybrid incompatibility loci (Sweigart and Flagel 2015), we generated a large *M. nasutus-M. guttatus* F_2 hybrid mapping population (N = 5487) and genotyped all individuals at gene-based markers flanking *hms1* (M8 and M24) and *hms2* (M51 and MgSTS193). As previously reported (Sweigart et al. 2006; Sweigart and Flagel 2015), we observed significant transmission ratio distortion (TRD) in F_2 genotypes at both hybrid sterility loci (Table 1). At *hms1*, we observed a significant excess of heterozygotes, but allelic transmission did not differ from the Mendelian expectation. The observed genotype ratios at *hms1* also differed significantly from the expectation given the random union of two gametes with the observed allele frequencies. At *hms2*, we observed an excess of *M. guttatus* homozygotes and a deficit of *M. nasutus* homozygous genotypes, as well as a significant bias toward *M. guttatus* alleles. However, genotype ratios at *hms2* do not differ from what is expected given the observed allele frequencies. Taken together, these patterns suggest TRD at *hms1* might be driven primarily by zygotic selection, whereas *hms2* appears to be influenced primarily by selection among gametes.

When considered together, the two-locus genotypes at *hms1* and *hms2* differ significantly from the Mendelian expectation (X^2 = 389.372, d.f. = 8, $P < 0.0001$, N = 5487). Although the two-locus genotypes are also significantly different from the expectation given the observed allele frequencies at *hms1* and *hms2* shown in Table 1 (X^2 = 71.626, d.f. = 8, P <0.0001), the values are much more closely aligned (Table 2). Particularly notable is the deficit of two genotypic classes ($hms1_{GG}$; $hms2_{NN}$ and $hms1_{NN}$; $hms2_{GG}$) and the excess of two others ($hms1_{GG}$; $hms2_{GG}$ and $hms1_{NN}$; $hms2_{NN}$; Table 2). This pattern of two-locus disequilibrium follows the expectation for gametic action of *hms1-2* sterility (*i.e.*, with $hms1_G$; $hms2_N$ gametes tending to be sterile). However, the observed F_2 transmission ratios at *hms1* and *hms2* cannot be entirely explained by $hms1_G$; $hms2_N$ gametic sterility (Table S1). This phenomenon, whether acting through one or both parents, would be expected to reduce the transmission of *M. guttatus* alleles at *hms1*, in the same way that it reduces *M. nasutus* alleles at *hms2*. However, there is no

343 indication of allelic transmission bias at *hms1* in the F_2 hybrids. Taken together, these
344 results suggest that gametic expression of the *hms1-hms2* incompatibility is important,
345 but not the sole contributor, to patterns of transmission ratio distortion in F_2 hybrids.
346
347 **_M. nasutus-M. guttatus_ IL crosses reveal multiple causes of F_2 distortion**
348 To investigate several possible causes of F_2 transmission ratio distortion at *hms1* and
349 *hms2*, we performed a crossing experiment using the IL-G and IL-Ns. In this crossing
350 design (Figure 1), individuals with one of several possible two-locus *hms1-hms2*
351 genotypes – in each of the IL genetic backgrounds – were crossed reciprocally to *M.*
352 *guttatus* (IM62) and *M. nasutus* (SF5). By scoring *hms1* and *hms2* genotypes in the
353 progeny of these crosses, we were able to examine the effects of several factors,
354 including parental genotype, genetic background, and cross direction, on transmission
355 ratios at the two hybrid sterility loci. Of the 36 crosses performed, 12 showed significant
356 transmission ratio distortion at *hms1* and/or *hms2* (Table 3; note that two crosses were
357 unsuccessful due to hybrid male sterility). For both *hms1* and *hms2*, parental genotype at
358 one locus has a strong effect on allelic transmission at the other (*hms1* affects *hms2*: F =
359 37.69, $P < 0.0001$; *hms2* affects *hms1*: $F = 7.80$, $P = 0.004$; Figure S1). For *hms2*, cross
360 direction is also important, with stronger TRD occurring through pollen ($F = 72.33$, $P <$
361 0.0001). Neither the genetic background nor the identity of the recurrent parent
362 significantly affected transmission ratios at *hms1* or *hms2* (results not shown).
363 The pattern of TRD at *hms2* follows what is expected if hybrid sterility acts
364 through gametes. For example, if pollen grains are inviable when they carry *M. guttatus*
365 alleles at *hms1* in combination with *M. nasutus* alleles at *hms2*, the effect of *hms1*
366 paternal genotype on TRD at *hms2* should be additive. Indeed, progeny from males that
367 carry one or two *M. guttatus* alleles at *hms1* show a 28% or 76% under-transmission of
368 *M. nasutus* alleles at *hms2* relative to the Mendelian expectation (Figure S1). Consistent
369 with the action of a gametic incompatibility, backcross progeny of doubly heterozygous
370 IL parents (*i.e.*, $hms1_{GN}$; $hms2_{GN}$) are much less likely to come from gametes with an *M.*
371 *guttatus* allele at *hms1* in combination with an *M. nasutus* allele at *hms2* (Table 4). In
372 these crosses, the $hms1_{G}$; $hms2_{N}$ gamete type is under-transmitted through both sexes,

though the effect is stronger through males. Under-transmission is also more severe in crosses to IM62 (*M. guttatus*) and against the IL-N genetic background (Table S2).

If the *hms1-hms2* incompatibility acts through gametes, we might expect patterns of pollen viability to predict rates of transmission ratio distortion through males. To examine this possibility, we measured pollen viability in various two-locus genotypes of the IL-G and IL-Ns (Table 5). In general, patterns of male fertility and transmission ratio distortion are indeed related. For example, pollen viability is 64% in IL-Gs that are $hms1_{GG}$; $hms2_{GN}$. For this genotype, if we assume equal transmission of *M. guttatus* and *M. nasutus* alleles into pollen and attribute all sterility to $hms1_{G}$; $hms2_{N}$, then the *M. guttatus* allele at *hms2* should be present in 78% of progeny when this individual is used as the paternal parent in a cross (which is close to the observed frequency of 86%, Table 3). Similarly, for IL-Gs that are $hms1_{GN}$; $hms2_{GN}$, if we assume that all $hms1_{G}$; $hms2_{N}$ gametes are inviable (and divide the remaining 7% sterility equally among the other three two-locus genotypes), we expect *M. guttatus* allele frequencies of 33% and 66% at *hms1* and *hms2*, respectively. These values are very similar to what we observe when this IL-G genotype is backcrossed to *M. guttatus* (37% and 67%, Table 3).

At *hms1*, TRD is more complex. On the one hand, *M. guttatus* alleles at *hms1* are under-transmitted due to the $hms1_{G}$; $hms2_{N}$ gametic sterility discussed above (Table S2). On the other hand, in many of the IL-backcrosses, *M. guttatus* alleles at *hms1* are overrepresented among the progeny (Tables 2 and 2.1). This effect is most pronounced when the IL parent is heterozygous at *hms1* and homozygous for *M. nasutus* alleles at *hms2* (Figure S1; note that this genotype is not completely sterile so crosses can still be performed). Remarkably, this direction of TRD is exactly the opposite of what is expected if *hms1* transmission is primarily influenced by the $hms1_{G}$; $hms2_{N}$ gametic incompatibility. Moreover, pollen viability in IL-G and IL-Ns with the genotype $hms1_{GN}$; $hms2_{NN}$ is much lower than the 50% expected for gametic expression of hybrid male sterility (Table 5), consistent with over-transmission of *M. guttatus hms1* alleles into pollen. Note that if these two TRD mechanisms – $hms1_{G}$; $hms2_{N}$ gamete sterility and over-transmission of *M. guttatus hms1* alleles – counteract each other in F_1 hybrids and in doubly heterozygous ILs, it could explain why their progeny carry *hms1* alleles in roughly Mendelian proportions (Table 2, Figure S1). Consistent with this idea, backcross

progeny of doubly heterozygous ILs are most often products of the *hms1*$_G$; *hms2*$_G$ gamete type (Table 4).

Additionally, a genetically distinct hybrid incompatibility appears to affect transmission of *hms1* against an *M. nasutus* genetic background. Self-fertilization of a doubly heterozygous IL-N individual produces no *M. guttatus* homozygotes at the *hms1* locus (Table 2), a genotype expected to appear in a quarter of the progeny (IL-N F_2 N = 200, expected frequency = 50). When instead this same doubly heterozygous IL-N genotype is crossed to IM62 (in either direction), progeny homozygous for *M. guttatus* alleles at *hms1* are recovered (Table S3). Note that selfing the doubly heterozygous IL-N produces offspring with isogenic *M. nasutus* genetic backgrounds, whereas the backcross to IM62 results in progeny with genetic backgrounds that are F_1-like. Taken together, these results suggest that the *hms1* region is involved in yet another hybrid incompatibility. This one causes lethality in hybrids that are homozygous for *M. guttatus* alleles at *hms1* (or linked loci) and homozygous for *M. nasutus* alleles at one or more unlinked loci.

By scoring genotype frequencies in the progeny of reciprocal backcrosses involving the doubly heterozygous ILs (*hms1*$_{GN}$; *hms2*$_{GN}$), it is possible to track which two-locus *hms1-2* meiotic products are transmitted through pollen and ovules. If we use these observed two-locus gametic allele frequencies (instead of assuming equal proportions of the four two-locus gamete types) to calculate expected genotype frequencies in the selfed progeny of doubly heterozygous ILs (i.e., IL-F_2 populations), the resulting values do not significantly differ from observed proportions (Table 2, Table 4). To fully account for observed genotype frequencies in the IL-N F_2, it is also necessary to assume complete lethality of *M. guttatus* homozygotes at *hms1* (Table 2; note that this hybrid lethality is not reflected in IL backcross allele frequencies because progeny do not carry the requisite *M. nasutus* genetic background for expression of the incompatibility).

In summary, we have identified at least three sources of *hms1-hms2* TRD in *M. nasutus-M. guttatus* F_2 hybrids: 1) under-transmission of pollen and, to a lesser extent, ovules that carry an *M. guttatus* allele at *hms1* in combination with an *M. nasutus* allele at *hms2*, presumably due to gametic inviability, 2) over-transmission of *M. guttatus* alleles at *hms1*, an effect that occurs through males and females, and does not depend on genetic

435 background, and 3) hybrid lethality in individuals homozygous for *M. guttatus* alleles at
436 *hms1* (and linked genomic regions) in combination with *M. nasutus* homozygosity at one
437 or more unlinked loci.
438
439 **Fine-mapping TRD**
440 In previous (Sweigart and Flagel 2015) and ongoing efforts to fine-map *hms1* and *hms2*,
441 we identified a small subset of SF5-IM62 F_2 hybrids that were recombinant for one or
442 both sets of *hms* flanking markers. With the goal of genetically mapping TRD in both
443 regions, we self-fertilized these recombinants to generate F_3 progeny and examined
444 genotype frequencies at both sets of flanking markers (Figures 3 and 4). We reasoned that
445 TRD in the F_3 progeny should only be observable if the causal locus is heterozygous in
446 the F_2 parent. If, instead, the TRD-causing locus is homozygous (for either *M. guttatus* or
447 M. *nasutus* alleles), loci in the adjacent heterozygous region should segregate in a
448 Mendelian fashion.
449 As in the IL crosses, patterns of *hms2*-linked TRD were consistent with the action
450 of $hms1_G$; $hms2_N$ gametic sterility. In this genomic region, the most extreme TRD
451 occurred in the two F_3 families that descended from F_2 hybrids with the $hms1_{GG}$; $hms2_{GN}$
452 genotype (Figure 2). Despite this general support for *hms1-hms2* gametic sterility, *hms2*-
453 linked TRD could not be unambiguously mapped to a particular genomic region (no
454 interval in Figure 2 is perfectly associated with presence/absence of TRD). Presumably,
455 genetic background in these F_2 hybrids can mask TRD associated with $hms1_G$; $hms2_N$
456 gametic sterility (*e.g.*, 28_22) or mimic it (*e.g.*, 02_66).
457 At *hms1*, the two contributors to TRD were decoupled in F_2 recombinants with *M.*
458 *guttatus* homozygotes overrepresented in some F_3 families and underrepresented in others
459 (Figure 3). As with the IL experiments, the most significant over-transmission of *M.*
460 *guttatus* alleles at *hms1* appears in the progeny of F_2 hybrids that are homozygous for *M.*
461 *nasutus* alleles at *hms2* (Figure 3, first two F_2s). This TRD phenotype maps to an 800-kb
462 region that includes *hms1*, but we have too few recombinants to determine if the hybrid
463 TRD phenotype is genetically separable from hybrid sterility. For a distinct set of *hms1*
464 F_2 recombinants, we observed a severe deficit of *M. guttatus* homozygotes among their
465 F_3 progeny (Figure 3, last six F_2 individuals), consistent with the expression of hybrid

lethality as seen in the IL experiments. This TRD phenotype maps to at least two independent loci in the *hms1* region and is not affected by *hms2* genotype, suggesting a distinct genetic basis for this hybrid incompatibility.

TRD at *hms1* within *M. guttatus*

To investigate whether *hms1*-linked TRD is a strictly hybrid phenomenon or also occurs within *M. guttatus*, we generated reciprocal F_2 progeny between IM62 and IM767. These two inbred lines carry distinct alleles at *hms1* and show very different patterns of variation in the surrounding genomic region. The IM62 line carries an incompatible, hybrid sterility-causing *hms1* allele embedded within a distinctive, 320-kb haplotype, whereas IM767 carries a compatible (*i.e.*, non-sterility causing) allele at *hms1* and typical levels of nucleotide variation in the region (Sweigart and Flagel 2015). Because genotype frequencies at *hms1* did not differ significantly between reciprocal F_2 populations (data not shown), we pooled data from both directions of the cross. We observed modest, but significant TRD at *hms1* with an excess of IM62 homozygotes (frequency of IM62 homozygotes to heterozygotes to IM767 homozygotes: expected 0.25:0.5:0.25, observed 00.27:0.54:0.19, $X^2 = 6.479$, d.f. = 2, $P = 0.0027$, $N = 582$). However, the bias in allelic transmission toward IM62 was not significant (frequency of IM62:IM767 alleles: expected 0.5:0.5, observed 0.54:0.46, $X^2 = 0.151$, d.f. = 1, $P < 0.151$, $N = 582$) and genotype frequencies did not significantly differ from the expectation given the allele frequencies ($X^2 = 2.025$, d.f. = 2, $P = 2.025$, $N = 582$). To further investigate the mechanism of *hms1*-linked TRD, we performed reciprocal backcrosses using IM62 and IM767. However, unlike in the IM62-IM767 F_2 hybrids, all four backcross populations exhibited nearly perfect Mendelian ratios (expected 0.50:0.50; F_1 x IM62 = 0.50:0.50, $N = 279$; F_1 x IM767 = 0.50:0.50, $N = 281$; IM62 x F_1 = 0.51:0.49, $N = 189$; IM767 x F_1 = 0.49:0.51, $N = 188$). These results suggest there is little to no transmission bias favoring the *hms1* incompatibility allele or the associated 320-kb haplotype within the Iron Mountain population.

Finally, we wanted to investigate if the presence of *M. nasutus* alleles at *hms2* increases the transmission bias of IM62 at *hms1* – even in an otherwise *M. guttatus* genetic background. To address this question, we examined genotype frequencies in the

reciprocal backcross progeny of individuals that were heterozygous IM62/IM767 at *hms1* and segregating for an *M. nasutus* introgression at *hms2* (against an otherwise IM62-IM767 F_2 genetic background; Figure S2). Indeed, extreme TRD at *hms1* (*i.e.*, bias toward the IM62 allele > 70%) was only observed in the backcross progeny of one individual (08_60) that was also homozygous for *M. nasutus* alleles at *hms2* (Table 6). These results suggest that over-transmission of the IM62 allele at *hms1*, which appears to require *M. nasutus* alleles at *hms2*, may occur exclusively in hybrids.

DISCUSSION

Transmission ratio distortion is commonly observed among hybrid offspring of recently diverged species, but the evolutionary significance is not always clear. In this study, we identified multiple contributors to hybrid TRD in genomic regions linked to two *Mimulus* hybrid sterility loci *hms1* and *hms2*, revealing a fine-scale complexity reminiscent of several previously characterized hybrid incompatibilities (Davis and Wu 1996; Long et al. 2008; Yang et al. 2012; Kubo et al. 2016b). We have discovered that hybrid transmission bias is caused, in part, by gametic action of the *hms1-hms2* incompatibility itself. However, the effects of the gametic hybrid sterility are partially obscured by an opposing (and currently unknown) mechanism that results in over-transmission of the *M. guttatus hms1* incompatibility allele in certain hybrid genetic backgrounds. In addition, our genetic analyses uncovered an independent hybrid lethality system with at least two incompatibility loci tightly linked to *hms1*. Strikingly, we found no evidence of biased transmission of the *hms1* incompatibility allele within *M. guttatus*, providing little support for selfish evolution as the cause of a recent, partial sweep at *hms1* (Sweigart and Flagel 2015). Instead, it appears that TRD at *hms1* and *hms2* might occur exclusively in hybrids.

Gametic action of *hms1-hms2* hybrid incompatibility

Our finding that the $hms1_G$; $hms2_N$ gamete type is severely under-transmitted in six of the eight backcrosses involving doubly heterozygous ILs ($hms1_{GN}$; $hms2_{GN}$) is strong evidence of gametic action of the incompatibility. This result runs counter to our previous

528 interpretation of the finding that pollen viability is reduced from the F_1 to F_2 generation,
529 which seemed to suggest a diploid (sporophytic) genetic basis for the *hms1-hms2*
530 incompatibility (Sweigart et al. 2006). In general, for a hybrid incompatibility that affects
531 the gametophyte, sterility is expected to be less severe in the F_2 generation due to the
532 inviability of recombinant F_1 gametes and regeneration of parental combinations.
533 However, in this case, it appears that removal of $hms1_G$; $hms2_N$ F_1 gametes is somewhat
534 balanced by over-transmission of *M. guttatus* alleles at *hms1*. Moreover, incomplete
535 penetrance of F_1 hybrid gametic sterility (*i.e.*, some $hms1_G$; $hms2_N$ gametes do contribute
536 to the F_2 generation, see Table 4) produces a small fraction of F_2 hybrids that are
537 completely sterile because they are homozygous for incompatible alleles (*i.e.*, $hms1_{GG}$;
538 $hms2_{NN}$).

539 As an independent line of evidence for gametic expression of the *hms1-hms2*
540 incompatibility, it is apparently difficult to introgress *M. nasutus hms2* alleles into an *M.*
541 *guttatus* genetic background. In the BG_4-NIL population (generated by four rounds of
542 backcrossing using IM62 as the pollen donor; see Methods from this study and Fishman
543 and Willis 2005), only 2.8% of individuals (5/175) are heterozygous at MgSTS45, a
544 marker ~2 cM from *hms2* (L. Fishman, unpublished results). This level of distortion is
545 notable: of the 194 markers genotyped in this BG_4 population, only four of them show
546 lower heterozygosity and three of those map near a meiotic drive locus that strongly
547 favors the *M. guttatus* allele (Fishman and Saunders 2008). In the BN_4 population
548 (generated by four rounds of backcrossing with SF5 as the pollen donor), heterozygous
549 introgressions at MgSTS45 are much more common, occurring in 10% of individuals (18
550 of 181). This result is not unexpected given that *M. guttatus* alleles at *hms2* are perfectly
551 compatible with *M. nasutus* alleles at *hms1*.

552 Unlike in animals, hybrid incompatibilities in plants are often gametic
553 (Morishima et al. 1991; Koide et al. 2008b; Leppala et al. 2013). Based on his studies of
554 hybrid sterility between the *indica* and *japonica* varieties of *Oryza sativa*, Oka (1974)
555 first suggested that defects in pollen development might be caused by loss-of-function
556 alleles at duplicate genes (Oka 1974). Indeed, two cases of this duplicate gametic lethal
557 model have now been demonstrated at the molecular level (Mizuta et al. 2010; Yamagata
558 et al. 2010). For *Mimulus hms1* and *hms2*, there's no evidence that gene duplicates are

559 involved (Sweigart and Flagel 2015), but a similar pattern of hybrid sterility is expected
560 to result from a two-locus hybrid incompatibility between any genes expressed in the
561 gametophyte. Additionally, the fact that the *hms1-hms2* incompatibility seems to affect
562 both the male and female gametophyte (the $hms1_G$; $hms2_N$ gamete type is under-
563 transmitted through both sexes) is consistent with our finding that these loci contribute to
564 both hybrid male sterility and hybrid female sterility (Sweigart et al. 2006). Gametic
565 hybrid incompatibilities that affect the fertility of both sexes have also been discovered in
566 tomato, rice, and *Arabidopsis* (Rick 1966; Koide et al. 2008a; Leppala et al. 2013),
567 though they are apparently less common than those that act in only one sex (Morishima et
568 al. 1991; Koide et al. 2008b)
569
570 **Additional sources of transmission ratio distortion**
571 Our fine-scale dissection of TRD at *hms1* and *hms2* provides insight into genomic
572 differentiation between closely related *Mimulus* species and reveals a potentially complex
573 genetic basis for hybrid dysfunction. In other systems, fine-mapping has often revealed
574 multiple, tightly linked hybrid incompatibility loci that show independent effects (Wu
575 and Davis 1993; Kubo et al. 2016a; Simon et al. 2016) or epistasis (Long et al. 2008;
576 Yang et al. 2012; Kubo et al. 2016b). In one particularly complex example from *indica*
577 and *japonica*, fine-mapping revealed two tightly linked genes involved in independent
578 two-locus pollen killer systems (Kubo et al. 2016b). Because of this tight linkage, pollen
579 killing had initially appeared to be caused by a single, three-locus interaction (Kubo *et al*.
580 2008). Remarkably, both of these pollen killer systems involve interactions between
581 sporophytic and gametophytic genes, as well as additional modifier loci (Kubo et al.
582 2016b). The picture emerging from such studies is one of hybrid sterility regulated by
583 multiple, interconnected molecular networks, potentially involving many genes.
584 A key question for *hms1* and *hms2* is whether the same genes cause the gametic
585 incompatibility and transmission bias of *M. guttatus* at *hms1*. The latter is particularly
586 strong when *hms2* is homozygous for *M. nasutus* alleles (Table 3, Figure S1), suggesting
587 it might be caused by an interaction between the two loci. Additionally, the presence of
588 $hms2_{NN}$ also appeared to unleash severe *hms1* TRD in one of the two IM62-IM767 F_2
589 populations in which it was present (Table 6), suggesting *hms2* might be necessary but

not sufficient for *hms1* TRD. On the other hand, over-transmission of $hms1_G$ does not seem to absolutely require $hms2_{NN}$ (*e.g.*, we observed 62% transmission of $hms1_G$ in *M. nasutus* x IL-$G_{GN;GG}$, Table 3), which might argue against its direct involvement. Indeed, for the IL-Gs, there is a bias toward $hms1_G$ in all backcross populations except those involving doubly heterozygous IL parents (*i.e.*, $hms1_{GN}$; $hms2_{GN}$), which, because they express the $hms1_G$; $hms2_N$ gametic inviability, might obscure additional sources of *hms1* TRD. Going forward, additional rounds of high-resolution fine-mapping will be needed to pinpoint the causal genes and determine if *Mimulus* hybrid sterility and TRD are genetically separable. Such efforts in rice have been successful in disentangling the complex phenotypic effects of linked hybrid sterility loci (*e.g.*, (Kubo et al. 2016a).

Identifying the molecular genetic basis of *hms1* TRD might also provide insight into its mechanisms. Because the bias toward *M. guttatus* alleles at *hms1* occurs through both males and females, the simplest single explanation is a gamete killing system that affects pollen and seeds. Alternatively, it is possible that independent mechanisms (and genetic loci) cause sex-specific TRD, such as pollen competition in males (*e.g.*, (Fishman et al. 2008)) and meiotic drive in females (*e.g.*, (Fishman and Saunders 2008). Whatever the cause, over-transmission of $hms1_G$ is apparently exacerbated by *M. nasutus* alleles at *hms2* to the point of overwhelming the effects of the $hms1_G$; $hms2_N$ gametic incompatibility. Indeed, the direction of TRD in the backcross progeny of $hms1_{GN}$; $hms2_{NN}$ ILs is counterintuitive: because of the $hms1_G$; $hms2_N$ gametic incompatibility, one expects transmission bias to be toward *M. nasutus* alleles. Instead, we observed exactly the opposite, namely, strong transmission bias toward *M. guttatus* at *hms1*. This finding might help explain < 50% pollen inviability in ILs with the genotype $hms1_{GN}$; $hms2_{NN}$. If $hms1_G$ alleles are highly overrepresented in pollen of such individuals due to gamete killing or some other mechanism, the gametic incompatibility will be expressed more often than expected under Mendelian inheritance. However, to explain the bias toward *M. guttatus* alleles in the backcross progeny, the gamete killing phenotype has to be stronger than the gametic incompatibility. In other words, some fraction of $hms1_G$; $hms2_N$ gametes must survive – and in greater numbers than $hms1_N$; $hms2_N$ gametes – to form zygotes. Clarifying the role of *hms2* in *hms1* TRD, and whether it acts through the

diploid sporophyte or haploid gametophyte, will be an important step toward understanding the mechanistic basis of hybrid distortion.

Surprisingly, our crossing experiments revealed at least two additional hybrid incompatibility loci linked to *hms1*. These loci, which contribute to TRD in the IL-Ns, appear to cause hybrid inviability and involve recessive alleles from both *Mimulus* species: against an *M. nasutus* genetic background, the *hms1* region cannot be made homozygous for *M. guttatus* alleles. The precise locations of these hybrid lethality loci are not yet known (Figure 3), but both potentially overlap with the 320-kb haplotype associated with the *hms1* incompatibility allele (Sweigart and Flagel 2015). This nearly invariant haplotype, which includes 30 genes, has recently risen to intermediate frequency in the Iron Mountain population of *M. guttatus*. The fact that multiple hybrid incompatibility loci are associated with this sweeping haplotype suggest that natural selection within a single population might have profound consequences for reproductive isolation between *Mimulus* species.

Implications for the evolution of hybrid sterility in *Mimulus*

An emerging theme in speciation genetics is that selfish evolution within species might be a major driver of hybrid incompatibilities. Decades of genetic analysis have provided a detailed mechanistic understanding of classic segregation distorters within *Drosophila* and mouse species (see (Presgraves 2008), and more recent studies have shown that hybrid sterility and hybrid TRD can be caused by the same genes (Phadnis and Orr 2009a; Zhang et al. 2015). However, very few studies have directly linked these two ends of the spectrum, testing whether incompatibility alleles act as selfish genetic elements within species. In one recent exception, Case *et al*. (2016) showed population genomic evidence for coevolution between a selfish cytoplasmic male sterility (CMS) gene and a nuclear restorer of fertility (*Rf* locus) within the Iron Mountain population of *M. guttatus* (Case et al. 2016). These same two loci also cause hybrid male sterility between *M. guttatus* and *M. nasutus*, suggesting that intragenomic conflict within Iron Mountain contributes to interspecific reproductive barriers.

Direct evidence for selfish evolution is missing from any of the hybrid gamete eliminators that have been cloned in rice (Long et al. 2008; Kubo et al. 2011; Yang et al.

2012; Kubo et al. 2016a; Kubo et al. 2016b; Yu et al. 2016). In most of these hybrid sterility systems, patterns of molecular variation at the causal genes in *japonica*, *indica*, and their wild ancestor *Oryza rufipogon* suggest that hybrid incompatibility alleles may never have expressed their killing phenotypes within species (*e.g.*, (Long et al. 2008; Yang et al. 2012),; also see (Sweigart and Willis 2012). In plants, it is also important to consider that even if gamete eliminators do arise within species and evolve selfishly to bias their own transmission, they might do so without any cost to individual fitness (Rick 1966). Especially for pollen killers, a sufficient number of viable pollen grains might still remain to fertilize all available ovules. Under a scenario of selfish evolution with no fitness costs, there is no conflict and, thus, no mechanism for generating hybrid incompatibilities.

Despite evidence for a recent selective sweep of the *hms1*-associated haplotype in the Iron Mountain population (Sweigart and Flagel 2015), our crossing experiments suggest there is no transmission bias favoring the IM62 *hms1* incompatibility allele. One caveat to this finding is that TRD at *hms1* might vary in different genetic backgrounds; even if there is no transmission bias between the IM62 and IM767 *hms1* alleles, TRD might occur in other heterozygous combinations. Alternatively, Iron Mountain individuals, including IM62 and IM762, might carry suppressors at *hms2*. However, given the recentness of the *hms1*-associated sweep (i.e. ~63 generations old; Sweigart and Flagel 2015), it seems unlikely that there has been sufficient time for a suppressor to evolve. Instead, *M. guttatus* from Iron Mountain and elsewhere may carry a "permissive" allele at *hms2* that allowed the evolution of the IM62 *hms1* variant without it expressing any transmission bias or sterility. Consistent with this idea, the incompatibility allele at *hms2* seems to be specific to *M. nasutus* (Sweigart et al. 2007), indicating this species likely carries the derived allele. Thus, instead of being driven by selfish evolution within *M. guttatus*, it appears that TRD at *hms1* is limited only to hybrids. These findings leave open the possibility that *hms1* evolution within Iron Mountain may have been driven by ecological adaptation. Further molecular characterization of these hybrid incompatibility loci and direct investigations of the fitness effects of alternative alleles at *hms1* will be important steps toward identifying the evolutionary causes of this reproductive barrier.

ACKNOWLEDGEMENTS

We thank Lila Fishman for sharing her BG_4 and BN_4 NILs and for valuable discussions. We are also grateful to Matt Zuellig who made thoughtful comments on an earlier draft, which improved the manuscript. We are especially indebted to Taylor Harrell and Rachel Hughes for expert greenhouse care and genotyping assistance. This work was supported by a National Science Foundation grant DEB-1350935 and funds from the University of Georgia Research Foundation to ALS.

REFERENCES

Barreau, C., E. Benson, E. Gudmannsdottir, F. Newton, and H. White-Cooper. 2008. Post-meiotic transcription in *Drosophila* testes. Development 135:1897-1902.

Brandvain, Y., A. M. Kenney, L. Flagel, G. Coop, and A. L. Sweigart. 2014. Speciation and introgression between *Mimulus nasutus* and *Mimulus guttatus*. PLoS genetics 10:e1004410.

Braun, R. E., R. R. Behringer, J. J. Peschon, R. L. Brinster, and R. D. Palmiter. 1989. Genetically haploid spermatids are phenotypically diploid. Nature 337:373-376.

Burt, A. and R. Trivers. 2006. Genes in conflict: the biology of selfish genetic elements. Harvard University Press, Cambridge, Massachusetts.

Cameron, D. R. and R. M. Moav. 1957. Inheritance in *Nicotiana tabacum* XXVII. Pollen killer, an alien genetic locus inducing abortion of microspores not carrying it.326-335.

Case, A. L., F. R. Finseth, C. M. Barr, and L. Fishman. 2016. Selfish evolution of cytonuclear hybrid incompatibility in *Mimulus*. Proceedings. Biological sciences / The Royal Society 283.

Case, A. L. and J. H. Willis. 2008. Hybrid male sterility in *Mimulus* (Phrymaceae) is associated with a geographically restricted mitochondrial rearrangement. Evolution; international journal of organic evolution 62:1026-1039.

Christie, P. and M. R. Macnair. 1987. The distribution of postmating reproductive isolating genes in populations of the yellow monkey flower, *Mimulus guttatus*. Evolution; international journal of organic evolution 41:571-578.

Crespi, B. and P. Nosil. 2013. Conflictual speciation: species formation via genomic conflict. Trends in ecology & evolution 28:48-57.

Davis, A. W. and C.-I. Wu. 1996. The broom of the sorcerer's apprentice: the fine structure of a chromosomal region causing reproductive isolation between two sibling species of *Drosophila*. Genetics 143:1287-1298.

Diaz, A. and M. R. Macnair. 1999. Pollen tube competition as a mechanism of prezygotic reproductive isolation between *Mimulus nasutus* and its presumed progenitor *M. guttatus*. The New phytologist 144:471-478.

724 Fishman, L., J. Aagaard, and J. C. Tuthill. 2008. Toward the evolutionary genomics of
725 gametophytic divergence: patterns of transmission ratio distortion in
726 monkeyflower (*Mimulus*) hybrids reveal a complex genetic basis for
727 conspecific pollen precedence. Evolution; international journal of organic
728 evolution 62:2958-2970.
729 Fishman, L. and A. Saunders. 2008. Centromere-associated female meiotic drive
730 entails male fitness costs in monkeyflowers. Science 322:1559-1561.
731 Fishman, L., A. L. Sweigart, A. M. Kenney, and S. Campbell. 2014. Major quantitative
732 trait loci control divergence in critical photoperiod for flowering between
733 selfing and outcrossing species of monkeyflower (*Mimulus*). The New
734 phytologist 201:1498-1507.
735 Fishman, L. and J. H. Willis. 2005. A novel meiotic drive locus almost completely
736 distorts segregation in *Mimulus* (monkeyflower) hybrids. Genetics 169:347-
737 353.
738 Frank, S. A. 1991. Divergence of meiotic drive-suppression systems as an
739 explanation for sex-biased hybrid sterility and inviability. Evolution;
740 international journal of organic evolution 45:262-267.
741 Gossmann, T. I., D. Saleh, M. W. Schmid, M. A. Spence, and K. J. Schmid. 2016.
742 Transcriptomes of plant gametophytes have a higher proportion of rapidly
743 evolving and young genes than sporophytes. Molecular biology and evolution
744 33:1669-1678.
745 Gossmann, T. I., M. W. Schmid, U. Grossniklaus, and K. J. Schmid. 2014. Selection-
746 driven evolution of sex-biased genes is consistent with sexual selection in
747 *Arabidopsis thaliana*. Molecular biology and evolution 31:574-583.
748 Hurst, L. D. and A. Pomiankowski. 1991. Causes of sex ratio bias may account for
749 unisexual sterility in hybrids: a new explanation of Haldane's Rule and
750 related phenomena. Genetics 128:841-858.
751 Johnson, N. A. 2010. Hybrid incompatibility genes: remnants of a genomic
752 battlefield? Trends in genetics : TIG 26:317-325.
753 Kenney, A. M. and A. L. Sweigart. 2016. Reproductive isolation and introgression
754 between sympatric *Mimulus* species. Molecular ecology 25:2499-2517.
755 Koide, Y., M. Ikenaga, N. Sawamura, D. Nishimoto, K. Matsubara, K. Onishi, A.
756 Kanazawa, and Y. Sano. 2008a. The evolution of sex-independent
757 transmission ratio distortion involving multiple allelic interactions at a single
758 locus in rice. Genetics 180:409-420.
759 Koide, Y., K. Onishi, A. Kanazawa, and Y. Sano. 2008b. Genetics of speciation in rice.
760 Rice Biology in the Genomics Era. Springer, Verlag Berlin Heidelberg.
761 Kubo, T. 2013. Genetic mechanisms of postzygotic reproductive isolation: An
762 epistatic network in rice. Breed Sci 63:359-366.
763 Kubo, T., T. Takashi, M. Ashikari, A. Yoshimura, and N. Kurata. 2016a. Two tightly
764 linked genes at the hsa1 locus cause both F1 and F2 hybrid sterility in rice.
765 Molecular plant 9:221-232.
766 Kubo, T., A. Yoshimura, and N. Kurata. 2011. Hybrid male sterility in rice is due to
767 epistatic interactions with a pollen killer locus. Genetics 189:1083-1092.

768 Kubo, T., A. Yoshimura, and N. Kurata. 2016b. Pollen killer gene S35 function
769 requires interaction with an activator that maps close to S24, another pollen
770 killer gene in rice. G3 6:1459-1468.
771 Leppala, J., F. Bokma, and O. Savolainen. 2013. Investigating incipient speciation in
772 *Arabidopsis lyrata* from patterns of transmission ratio distortion. Genetics
773 194.
774 Loegering, W. Q. and E. R. Sears. 1963. Distorted inheritance of stem-rust resistance
775 of Timstein wheat caused by a pollen-killing gene. Canadian Journal of
776 Genetics and Cytology 5:65-72.
777 Long, Y., L. Zhao, B. Niu, Su, J., H. Wu, Y. Chen, Zhang, Q., J. Guo, C. Zhuang, M. Mei, and
778 J. Xia. 2008. Hybrid male sterility in rice controlled by interaction between
779 divergent alleles of two adjacent genes. PNAS 105:18871-18876.
780 Lynch, M. and A. G. Force. 2000. The origin of interspecific genomic incompatibility
781 via gene duplication. American Naturalist 156:590-605.
782 Maheshwari, S. and D. A. Barbash. 2011. The genetics of hybrid incompatibilities.
783 Annu Rev Genet 45:331-355.
784 Martin, N. H. and J. H. Willis. 2007. Ecological divergence associated with mating
785 system causes nearly complete reproductive isolation between sympatric
786 *Mimulus* species. Evolution; international journal of organic evolution 61:68-
787 82.
788 Martin, N. H. and J. H. Willis. 2010. Geographical variation in postzygotic isolation
789 and its genetic basis within and between two *Mimulus* species. Philosophical
790 transactions of the Royal Society of London. Series B, Biological sciences
791 365:2469-2478.
792 McDermott, S. R. and M. A. Noor. 2010. The role of meiotic drive in hybrid male
793 sterility. Philosophical transactions of the Royal Society of London. Series B,
794 Biological sciences 365:1265-1272.
795 Mizuta, Y., Y. Harushima, and N. Kurata. 2010. Rice pollen hybrid incompatibility
796 caused by reciprocal gene loss of duplicated genes. PNAS 107:20417-20422.
797 Morishima, H., Y. Sano, and H.-I. Oka. 1991. Sterility barriers developed between and
798 within taxa. Pp. 159-166. Evolutionary studies in rice.
799 Oka, H.-I. 1974. Analysis of genes controlling F, sterility in rice by the use of isogenic
800 lines. Genetics 77:521-534.
801 Ouyang, Y. and Q. Zhang. 2013. Understanding reproductive isolation based on the
802 rice model. Annual review of plant biology 64:111-135.
803 Phadnis, N. and H. A. Orr. 2009a. A single gene causes both male sterility and
804 segregation distortion in *Drosophila* hybrids. Science 323:376-378.
805 Phadnis, N. and H. A. Orr. 2009b. A Single Gene Causes Both Male Sterility and
806 Segregation Distortion in *Drosophila* HybridsA Single Gene Causes Both Male
807 Sterility and Segregation Distortion in Drosophila Hybrids. Science 323:376-
808 378.
809 Presgraves, D. 2008. Drive and sperm: the evolution and genetics of male meiotic
810 drive.471-506.
811 Presgraves, D. C. 2010. The molecular evolutionary basis of species formation.
812 Nature reviews. Genetics 11:175-180.

Rick, C. M. 1966. Abortion of male and female gametes in the tomato determined by allelic interaction. Genetics 53:85-96.

Rutley, N. and D. Twell. 2015. A decade of pollen transcriptomics. Plant Reprod 28:73-89.

Sano, Y. 1990. The genic nature of gamete eliminator in rice. Genetics 125:183-191.

Schluter, D. and G. L. Conte. 2009. Genetics and ecological speciation PNAS 106:9955-9962.

Simon, M., S. Durand, N. Pluta, N. Gobron, L. Botran, A. Ricou, C. Camilleri, and F. Budar. 2016. Genomic conflicts that cause pollen mortality and raise reproductive barriers in *Arabidopsis thaliana*. Genetics 203:1353-1367.

Sweigart, A. L., L. Fishman, and J. H. Willis. 2006. A simple genetic incompatibility causes hybrid male sterility in *Mimulus*. Genetics 172:2465-2479.

Sweigart, A. L. and L. E. Flagel. 2015. Evidence of natural selection acting on a polymorphic hybrid incompatibility locus in *Mimulus*. Genetics 199:543-554.

Sweigart, A. L., A. R. Mason, and J. H. Willis. 2007. Natural variation for a hybrid incompatibility between two species of *Mimulus*. Evolution; international journal of organic evolution 61:141-151.

Sweigart, A. L. and J. H. Willis. 2003. Patterns of nucleotide diversity in two species of *Mimulus* are affected by mating system and asymmetric introgression. Evolution; international journal of organic evolution 57:2490-2506.

Sweigart, A. L. and J. H. Willis. 2012. Molecular evolution and genetics of postzygotic reproductive isolation in plants. F1000 biology reports 4:23.

Tao, Y., D. L. Hartl, and C. C. Laurie. 2001. Sex-ratio segregation distortion associated with reproductive isolation in *Drosophila*Sex-ratio segregation distortion associated with reproductive isolation in Drosophila. PNAS 98:13183-13188.

Vickery, R. K. J. 1978. Case studies in the evolution of species complexes in *Mimulus*. Evolutionary Biology 11:405-507.

Walbot, V. and M. M. Evans. 2003. Unique features of the plant life cycle and their consequences. Nature reviews. Genetics 4:369-379.

Werth, C. R. and M. D. Windham. 1991. A model for divergent, allopatric speciation of polyploid pteridophytes resulting from silencing of duplicate-gene expression. Am Nat 137:515-526.

Wu, C.-I. and A. W. Davis. 1993. Evolution of postmating reproductive isolation: the composite nature of haldane's rule
and its genetic bases. Am Nat 142:187-212.

Wuest, S. E., K. Vijverberg, A. Schmidt, M. Weiss, J. Gheyselinck, M. Lohr, F. Wellmer, J. Rahnenfuhrer, C. von Mering, and U. Grossniklaus. 2010. *Arabidopsis* female gametophyte gene expression map reveals similarities between plant and animal gametes. Current biology : CB 20:506-512.

Yamagata, Y., E. Yamamoto, K. Aya, K. T. Win, K. Doi, Sobrizal, T. Ito, H. Kanamori, J. Wu, T. Matsumoto, M. Matsuoka, M. Ashikari, and A. Yoshimura. 2010. Mitochondrial gene in the nuclear genome induces reproductive barrier in rice. Proceedings of the National Academy of Sciences of the United States of America 107:1494-1499.

Yang, J., X. Zhao, K. Cheng, H. Du, Y. Ouyang, J. Chen, S. Qiu, J. Huang, Y. Jiang, L. Jiang, J. Ding, J. Wang, C. Xu, X. Li, and Q. Zhang. 2012. A killer-protector system

regulates both hybrid sterility and segregation distortion in rice. Science 337:1336-1340.

Yu, Y., Z. Zhao, Y. Shi, H. Tian, L. Liu, X. Bian, Y. Xu, X. Zheng, L. Gan, Y. Shen, C. Wang, X. Yu, C. Wang, X. Zhang, X. Guo, J. Wang, H. Ikehashi, L. Jiang, and J. Wan. 2016. Hybrid sterility in rice (*Oryza sativa* L.) involves the tetratricopeptide repeat domain containing protein. Genetics 203:1439-1451.

Zhang, L., T. Sun, F. Woldesellassie, H. Xiao, and Y. Tao. 2015. Sex ratio meiotic drive as a plausible evolutionary mechanism for hybrid male sterility. PLoS genetics 11:e1005073.

Table 1. Genotype and allele frequencies at *hms1* and *hms2* in an *M. nasutus-M. guttatus* F_2 population (N = 5487).

	Allele frequency[1]	Genotype frequency[2]	
locus	O	O	E
hms1	0.49:0.51	0.22:0.55:0.23****	0.24:0.50:0.26
hms2	0.62:0.38****	0.38:0.48:0.14	0.38:0.47:0.14

[1] Observed (O) allele frequencies are reported as *M. guttatus*:*M. nasutus* (G:N). At *hms2*, but not *hms1*, allele frequencies significantly differ from the Mendelian expectation (0.5:0.5).

[2] Observed (O) and expected (E) genotype frequencies are reported as *M. guttatus* homozygotes:heterozygotes:*M. nasutus* homozygotes (GG:GN:NN). Expected genotype frequencies shown are calculated from the random union of gametes with the observed frequencies. At *hms1*, genotypes differ significantly ($P < 0.0001$) from both the Mendelian expectation (0.25:0.5:0.25) and from the expectation given the random union of gametes with the observed allele frequencies. At *hms2*, genotypes differ significantly ($P < 0.0001$) from the Mendelian expectation but not from the expectation given the random union of gametes with the observed allele frequencies.

**** $P < 0.0001$ based on X^2 tests of observed frequencies versus the Mendelian expectation with 2 d. f. for genotypes and 1 d. f. for allele frequencies.

Table 2. Observed and expected genotype frequencies at *hms1* and *hms2* in F_2 hybrids and IL F_2 hybrids.

genotype *hms1*; *hms2*	F_2 (5487)[1]			IL-G F_2 (167)[2]		IL-N F_2 (200)[3]		
	E: Mendelian	E: obs allele freqs	O	O	E: backcross	O	E: backcross	E: $hms1_{GG}$ = lethal
GG; GG	0.0625	0.093	0.099	0.066	0.107	0	0.119	0
GG; GN	0.1250	0.115	0.100	0.114	0.106	0	0.069	0
GG; NN	0.0625	0.035	0.022	0.006	0.200	0	0.090	0
GN; GG	0.1250	0.191	0.208	0.174	0.176	0.185	0.193	0.241
GN; GN	0.2500	0.236	0.268	0.234	0.249	0.300	0.249	0.310
GN; NN	0.1250	0.073	0.071	0.054	0.078	0.075	0.058	0.073
NN; GG	0.0625	0.098	0.070	0.102	0.072	0.085	0.077	0.096
NN; GN	0.1250	0.121	0.117	0.180	0.133	0.225	0.151	0.188
NN; NN	0.0625	0.037	0.047	0.072	0.061	0.130	0.0740	0.092

[1]F_2 genotype counts significantly differ from the Mendelian expectation (X^2 = 389.372, d.f. = 8, P <0.0001) and from what is expected for the random union of gametes given the observed allele frequencies (see Table 1) and independent assortment at *hms1* and *hms2* (X^2 = 71.626, d.f. = 8, P <0.0001).

[2]IL-G F_2 genotype counts significantly differ from the Mendelian expectation (X^2 = 18.7910, d.f. = 8, P = 0.0160), but not from what is expected based on allelic transmission in the IL backcrosses (see Table 4, X^2 = 5.9730, d.f. = 8, P = 0.6502).

[3]IL-N F_2 genotypes significantly differ from the Mendelian expectation (X^2 = 86.4090, d.f. = 8, P <0.0001) and from what is expected based on allelic transmission in the IL backcrosses (see Table 4, X^2 = 62.0370, d.f. = 8, P <0.0001), but not from what is expected from the IL backcrosses + $hms1_{GG}$ homozygote death (X^2 = 3.5950, d.f. = 5, P =0.6090).

Table 3. Allelic transmission ratios at *hms1* and *hms2* in IL backcross progeny.

♀[1]	♂	*hms1*; *hms2*[2]	*N*[3]	*hms1* %G[4]	*hms2* %G[5]
IL-G	G	GN; GG	101	0.56	
		GN; NN	171	0.60	
		GG; GN	163		0.53
		NN; GN	158		0.47
		GN; GN	293	0.46	0.54
IL-G	N	GN; GG	189	0.55	
		GN; NN	119	0.64*	
		GG; GN	49		0.53
		NN; GN	132		0.50
		GN; GN	232	0.52	0.54
G	IL-G	GN; GG	382	0.55	
		GN; NN	no seeds	--	
		GG; GN	120		0.86****
		NN; GN	187		0.50
		GN; GN	298	0.37***	0.67****
N	IL-G	GN; GG	636	0.62****	
		GN; NN	no seeds	--	
		GG; GN	158		0.90****
		NN; GN	187		0.52
		GN; GN	450	0.53	0.64****
IL-N	G	GN; GG	266	0.44	
		GN; NN	593	0.48	
		GG; GN	n/a		--
		NN; GN	325		0.55
		GN; GN	354	0.42*	0.59*
IL-N	N	GN; GG	211	0.48	
		GN; NN	317	0.52	
		GG; GN	n/a		--
		NN; GN	43		0.54
		GN; GN	320	0.58*	0.66****
G	IL-N	GN; GG	113	0.46	
		GN; NN	85	0.71**	
		GG; GN	n/a		--
		NN; GN	250		0.53
		GN; GN	104	0.37*	0.64*
N	IL-N	GN; GG	177	0.51	
		GN; NN	194	0.72****	
		GG; GN	n/a		--
		NN; GN	188		0.57
		GN; GN	212	0.42	0.61*

[1]Backcrosses using ILs (*M. guttatus* background = IL-G; *M. nasutus* background = IL-N) to the IM62 line of *M. guttatus* (G) and the SF5 line of *M. nasutus* (N). ♀ indicates the maternal parent and ♂ indicates the paternal parent.

[2]Two-locus genotype for *hms1* and *hms2*. GG = *M. guttatus* homozygote; GN = heterozygote; NN = *M. nasutus* homozygote.

[3]Number of progeny assessed. Two crosses were unsuccessful (labeled "no seeds") because the IL-G with the genotype $hms1_{GN}$; $hms2_{NN}$ was completely male sterile. The IL-N with the genotype $hms1_{GG}$; $hms2_{GN}$ could not be generated (see text) and is labeled "n/a."

[4]Percent *M. guttatus* (G) alleles at *hms1* transmitted to progeny from heterozygous IL parent.

[5]Percent *M. guttatus* (G) alleles at *hms2* transmitted to progeny from heterozygous IL parent.

* $P < 0.05$, ** $P < 0.01$, *** $P < 0.005$, **** $P < 0.0001$ based on X^2 tests of observed frequencies versus the Mendelian expectation.

Table 4. Two-locus transmission ratios at *hms1* and *hms2* in backcross progeny of doubly heterozygous ILs.

			hms1;hms2[3]				
♀[1]	♂	*N*[2]	G;G	G;N	N;G	N;N	*P*
IL-G	G	293	0.31	0.20	0.24	0.25	
IL-G	N	232	0.28	0.24	0.25	0.22	
IL-N	G	354	0.30	0.13	0.30	0.28	***
IL-N	N	320	0.43	0.15	0.22	0.19	****
average			0.33	0.18	0.25	0.24	
G	IL-G	298	0.32	0.05	0.35	0.28	****
N	IL-G	450	0.40	0.13	0.24	0.23	****
G	IL-N	104	0.34	0.03	0.30	0.34	****
N	IL-N	212	0.32	0.10	0.30	0.29	***
average			0.34	0.08	0.30	0.28	

[1]Backcrosses using ILs (*M. guttatus* background = IL-G; *M. nasutus* background = IL-N) to the IM62 line of *M. guttatus* (G) and the SF5 line of *M. nasutus* (N). ♀ indicates the maternal parent and ♂ indicates the paternal parent.
[2]Number of progeny assessed.
[3]Two-locus allelic combination at *hms1* and *hms2* inherited from IL parent. G = *M. guttatus* allele; N = *M. nasutus* allele.
* $P < 0.05$, ** $P < 0.01$, *** $P < 0.005$, **** $P < 0.0001$ based on X^2 tests of observed frequencies versus the Mendelian expectation.

Table 5. Pollen viability for various *hms1-2* IL genotypes.

Genetic Background	*hms1*; *hms2*	*N*[1]	PV[2]
IL-G	GG; GN	5	0.64 (0.04)
	NN; GN	16	0.79 (0.04)
	GN; GN	16	0.67 (0.06)
	GN; GG	12	0.71 (0.06)
	GN; NN	3	0.18 (0.17)
IL-N	NN; GN	15	0.88 (0.02)
	GN; GN	14	0.81 (0.03)
	GN; GG	13	0.85 (0.02)
	GN; NN	18	0.09 (0.01)

[1]Number of individuals scored.
[2]Pollen viability given as the proportion viable pollen grains per flower (for a haphazard sample of 100). PV is the average of two flowers and the number in parentheses is the standard error.

Table 6. Transmission of IM62 vs. IM767 at *hms1* varies depending on *hms2* genotype.

hms2 genotype	F_2 ID[1]	%IM62[2]	
		F_2 male	F_2 female
IM62	02_02	0.58 (74)	0.55 (64)
	02_46	0.48 (121)	0.43 (28)
	06_31	0.55 (179)	0.29 (41)
	06_70	0.55 (123)	0.50 (116)
	06_96	0.41 (46)	--
	combined	0.53 (543)	0.47 (249)
IM767	02_17	0.45 (53)	0.56 (122)
	02_48	0.54 (79)	0.49 (84)
	02_68	0.56 (39)	0.49 (141)
	06_39	0.55 (107)	--
	combined	0.53 (278)	0.51 (347)
SF	08_60	0.77 (104)****	0.73 (75)***
	12_09	0.50 (111)	0.54 (41)
	combined	0.62 (215)**	0.66 (116)*

[1]Individual IDs for F_2 progeny from $BG_4$275-IM767 crosses. At *hms1*, all F_2 individuals used were heterozygous for IM62 and IM767 alleles; at *hms2*, individuals used were homozygous for IM62, IM767, or SF alleles (see text for details).

[2]Percent IM62 alleles at *hms1* transmitted to progeny from IM62-IM767 heterozygous parent. Value given in parentheses is the number of progeny assessed.

* $P < 0.05$, ** $P < 0.01$, *** $P < 0.005$, **** $P < 0.0001$ based on X^2 tests of observed genotype frequencies versus the Mendelian expectation.

Figure 1

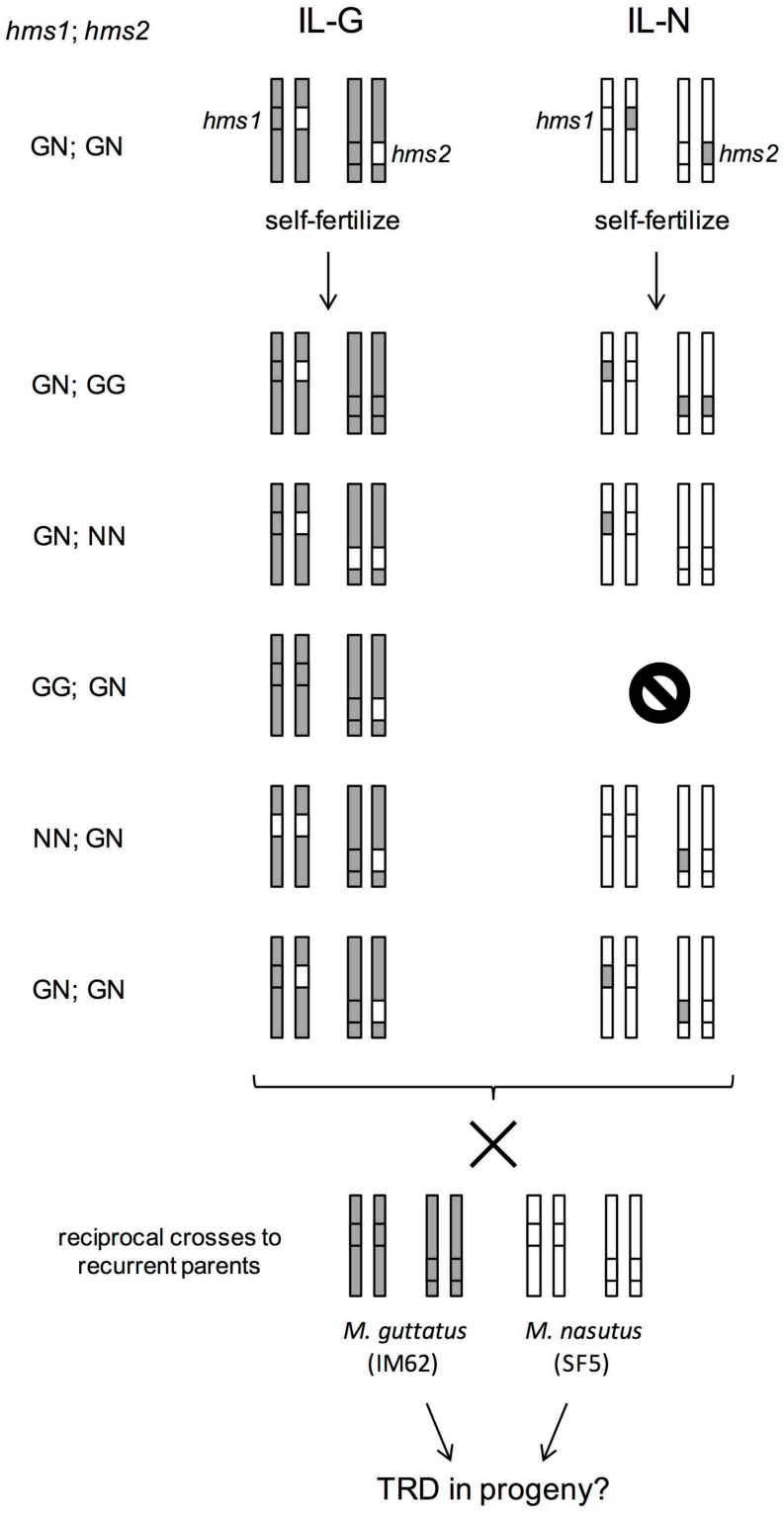

Figure 1. Crossing design for backcross experiment using introgression lines (ILs). For each genotype, two chromosome pairs are shown (one with *hms1* and one with *hms2*). We constructed two sets of ILs with heterozygous introgressions at both *hms1* and *hms2*; the IL-G has an *M. guttatus* genetic background (grey shading) and the IL-N has an *M. nasutus* genetic background (white). These doubly heterozygous ILs were self-fertilized to generate progeny with two-locus genotypes that are heterozygous at *hms1* and/or *hms2*. These five progeny types were then reciprocally backcrossed to *M. guttatus* and *M. nasutus*. G = *M. guttatus* allele (grey) ; N = *M. nasutus* allele (white).

Figure 2

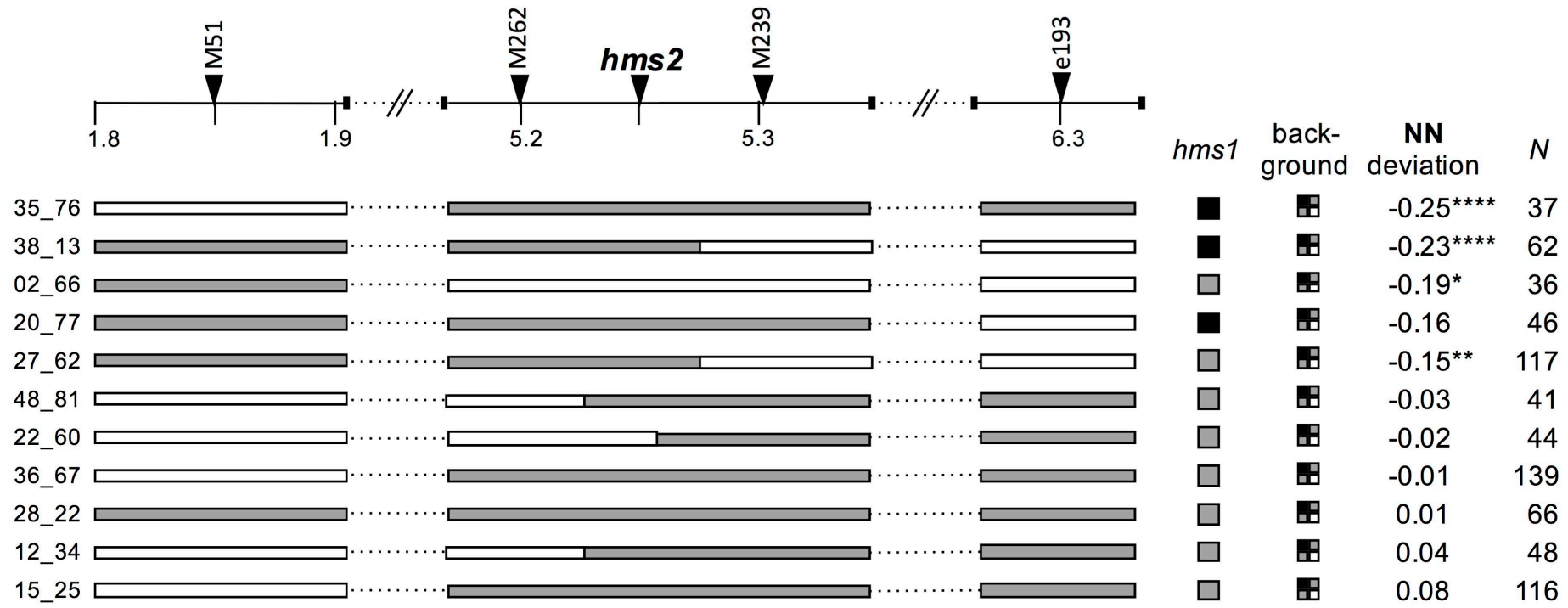

Figure 2. Genetic dissection of *hms2*-linked TRD in *Mimulus*. A physical map of ~4.5 Mb the *hms2* region is shown, including the positions of genetic markers (indicated with triangles along the top). F_2 recombinants are shown with horizontal bars representing genotypes in the genomic region linked to *hms2* and squares indicating genotypes at *hms1* and across the genetic background (white = *M. nasutus* homozygote, grey = heterozygote, black = *M. guttatus* homozygote). Deviation from the Mendelian expectation (0.25) of *M. nasutus* homozygotes (NN) in the F_3 progeny is given. *N* indicates the number of F_3 progeny scored from each individual. * $P < 0.05$, ** $P < 0.01$, *** $P < 0.005$, **** $P < 0.0001$ based on X^2 tests of observed frequencies versus the Mendelian expectation.

Figure 3

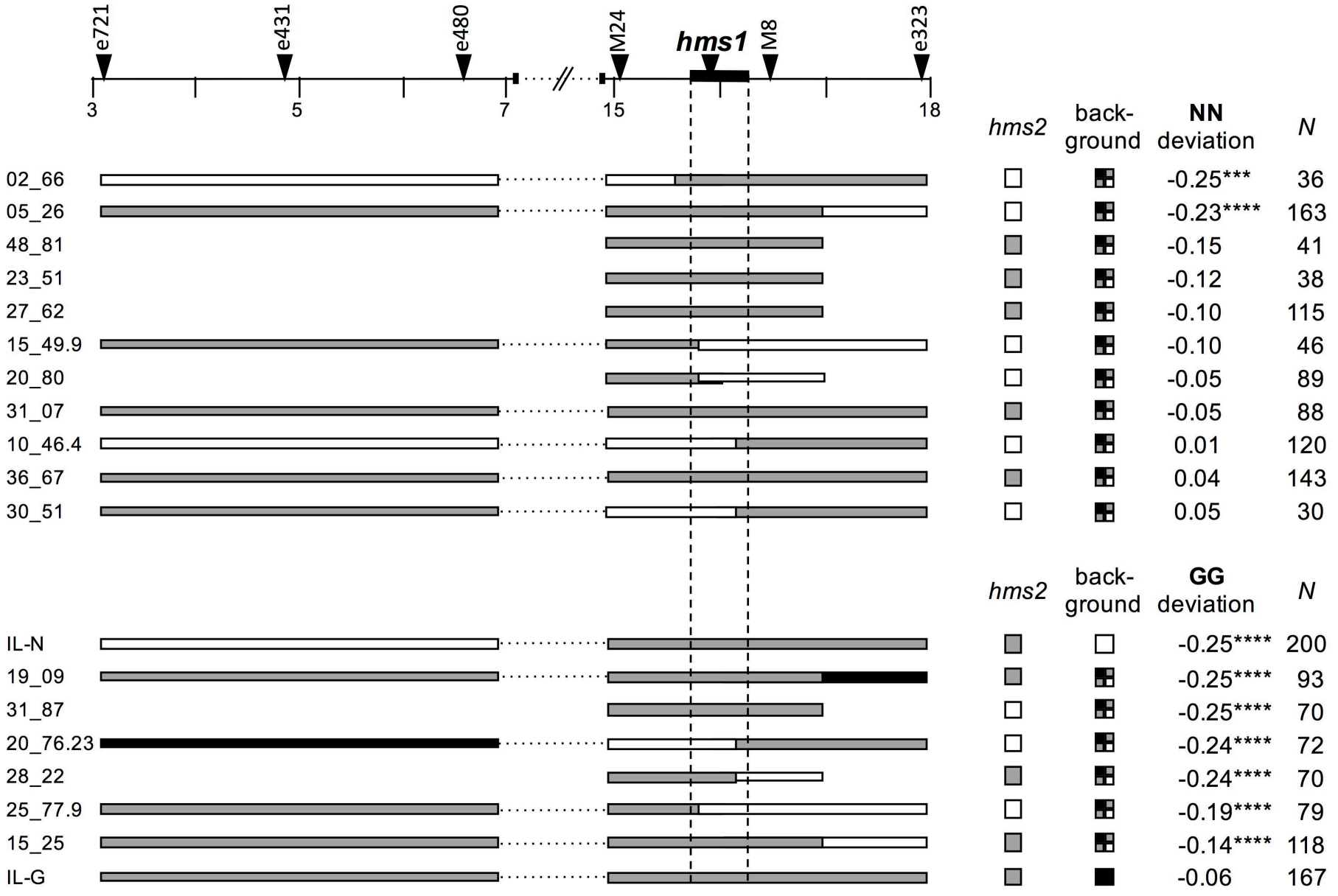

Figure 3. Genetic dissection of *hms1*-linked TRD in *Mimulus*. A physical map of 15 Mb the *hms1* region is shown, including the positions of genetic markers (indicated with triangles along the top) and the 320-kb *hms1* haplotype (shown as a solid black bar with dotted lines extending downwards). F_2 recombinants are shown with horizontal bars representing genotypes in the genomic region linked to *hms1* and squares indicating genotypes at *hms2* and across the genetic background (white = *M. nasutus* homozygote, grey = heterozygote, black = *M. guttatus* homozygote). Deviation from the Mendelian expectation (0.25) of *M. nasutus* homozygotes (NN) in the F_3 progeny is given for the top group of 11 F_2 recombinants. Deviation from the Mendelian expectation (0.25) of *M. guttatus* homozygotes (GG) in the F_3 progeny is given for the bottom group of six F_2 recombinants and the doubly heterozygous ILs. *N* indicates the number of F_3 progeny scored from each individual. *** $P < 0.005$, **** $P < 0.0001$ based on X^2 tests of observed frequencies versus the Mendelian expectation.

Figure S1

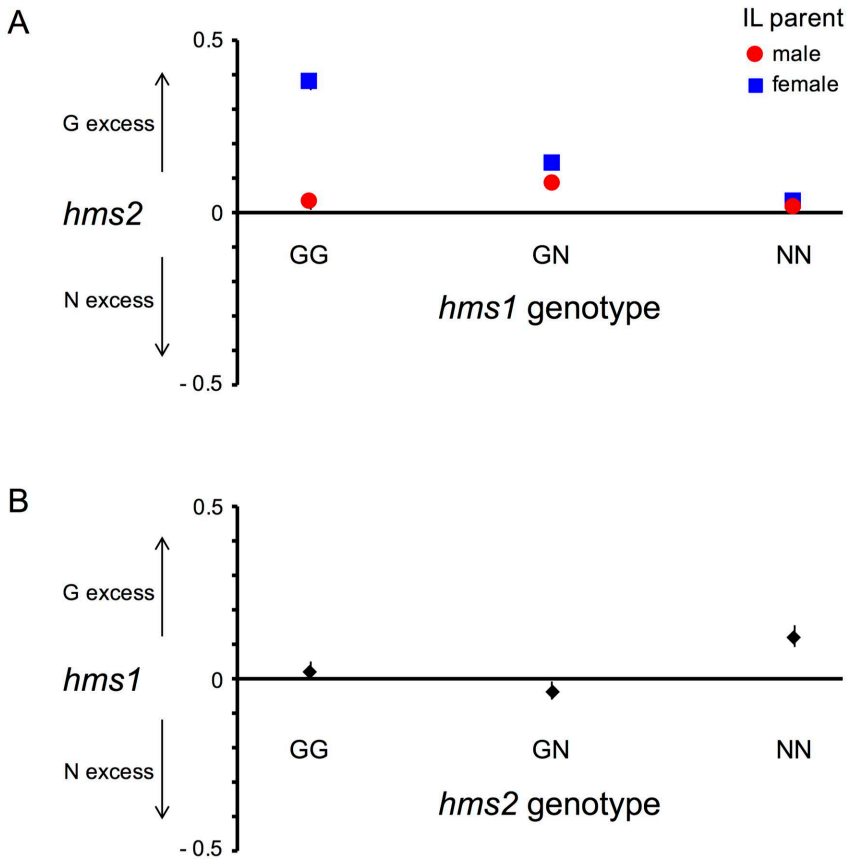

Figure S1. Transmission ratio distortion at *hms1* and *hms2* in IL-backcross progeny. The vertical position of each symbol shows the magnitude and direction of the deviation of allelic transmission from the Mendelian expectation (0.5). *M. guttatus* deviations are graphed directly [deviation = *f*(N – 0.5)], and the *M. nasutus* deviations are graphed as negative [deviation = - (*f*(N-0.25)]. Thus, values above zero indicate excess of *M. guttatus* alleles and values below zero indicate excess of *M. nasutus* alleles. G = *M. guttatus* allele, N = *M. nasutus* allele. A) Allelic transmission of *hms2* in the progeny of IL-backcrosses is significantly affected by IL parental genotype at *hms1* ($F = 37.6919$, $P < 0.0001$), cross direction ($F = 72.3339$, $P < 0.0001$), and their interaction ($F = 31.8353$, $P < 0.0001$). B) Allelic transmission of *hms1* in the progeny of IL-backcrosses is significantly affected by IL parental genotype at *hms1* ($F = 7.7977$, $P = 0.0043$).

Figure S2

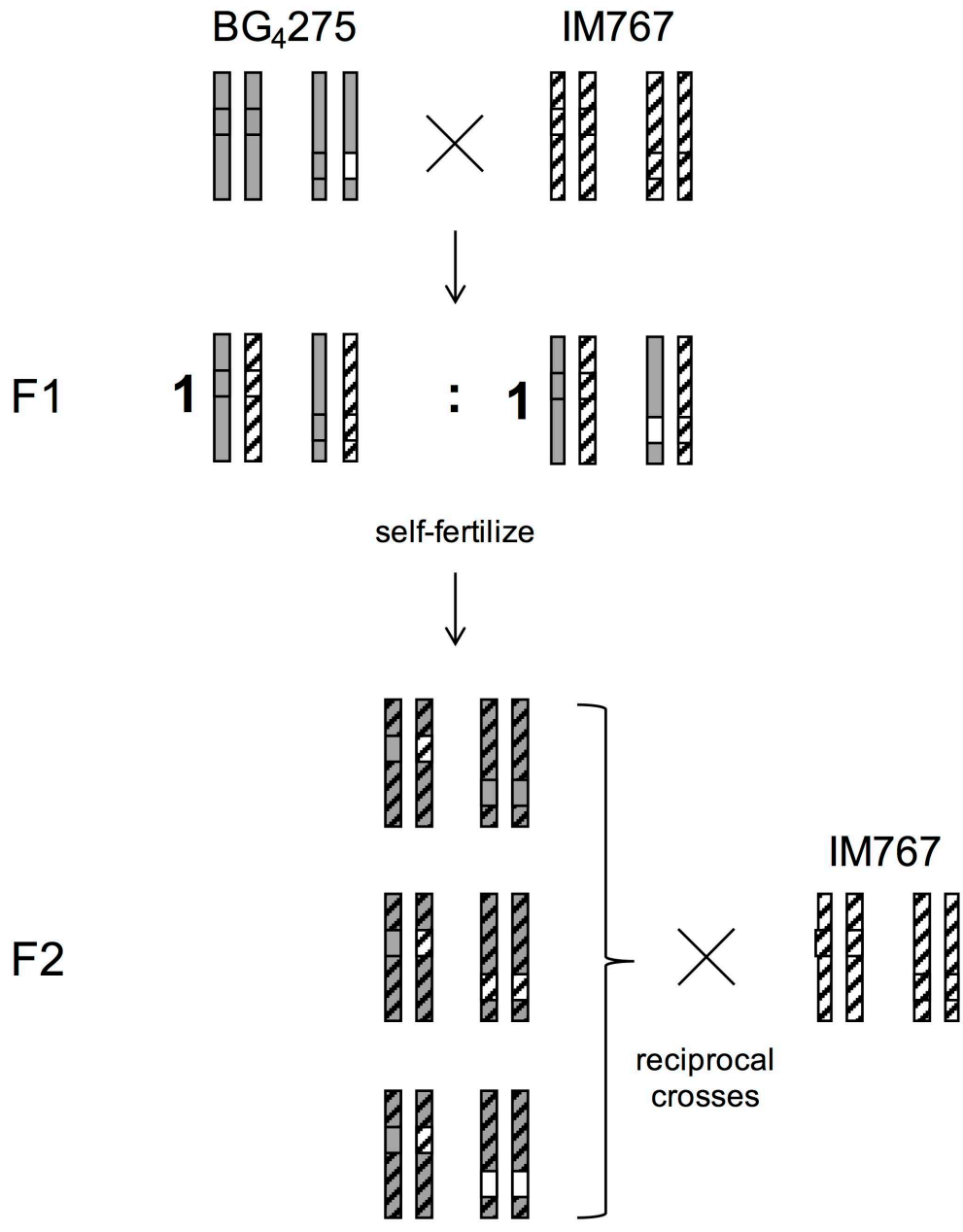

Figure S2. Crossing scheme for investigating the effect of *M. nasutus* (SF5) homozygosity at *hms2* on within-*M. guttatus* TRD at *hms1*. For each genotype, two chromosome pairs are shown (one with *hms1* and one with *hms2*). We intercrossed IM767 (stripes) and BG_4.275, which carries a heterozygous SF5 introgression (white) at *hms2* against an IM62 (grey shading) genetic background. The resulting progeny segregate 1:1 for two different genotypes at *hms2*: IM62-IM767 heterozygotes and SF5-IM767 heterozygotes (the remaining genetic background is heterozygous for IM62 and IM767 alleles). We genotyped F_2 progeny with *hms*-linked markers to identify IM62-IM767 *hms1* heterozygotes in combination with three different *hms2* genotypes: IM62 homozygotes, IM767 homozygotes, and SF5 homozygotes. Individuals with each of these three two-locus genotypes were then reciprocally backcrossed to IM767 to assess TRD at *hms1*. Note that the genetic background of the F_2 progeny are expected to segregate 1:2:1 for IM62 homozygotes, heterozygotes, and IM767 homozygotes (grey shading with stripes).

Table S1. Observed and expected genotype frequencies at *hms1* and *hms2* in F_2 hybrids (N = 5487).

genotype *hms1*; *hms2*	O	E: Mendelian	E: GN inviable, 1 parent[1]	E: GN inviable, 2 parents[2]	E: GN partial inviablity, 1 parent[3]
GG; GG	0.099	0.0625	0.083	0.109	0.076
GG; GN	0.100	0.1250	0.083	0	0.098
GG; NN	0.022	0.0625	0	0	0.022
GN; GG	0.208	0.1250	0.165	0.218	0.152
GN; GN	0.268	0.2500	0.248	0.218	0.25
GN; NN	0.071	0.1250	0.083	0	0.098
NN; GG	0.070	0.0625	0.083	0.109	0.076
NN; GN	0.117	0.1250	0.165	0.218	0.152
NN; NN	0.047	0.0625	0.083	0.109	0.076

[1] Expected F_2 genotype frequencies if 100% of $hms1_G$; $hms2_N$ gametes are inviable in one parent. Observed F_2 genotype counts significantly differ from this expectation (X^2 = 325.725, d.f. = 8, P <0.0001). G = *M. guttatus* allele, N = *M. nasutus* allele.
[2] Expected F_2 genotype frequencies if 100% of $hms1_G$; $hms2_N$ gametes are inviable in both parents. Observed F_2 genotype counts significantly differ from this expectation (X^2 = 1853.55, d.f. = 8, P <0.0001).
[3] Expected F_2 genotype frequencies if 65% of $hms1_G$; $hms2_N$ gametes are inviable in one parent. This threshold of inviability was set by assuming the observed $hms1_{GG}$; $hms2_{NN}$ F_2 genotype frequency was determined solely by partial inviability through one parent. Observed F_2 genotype counts significantly differ from this expectation (X^2 = 156.892, d.f. = 8, P <0.0001).

Table S2. The severity of under-transmission of *hms1*$_G$; *hms2*$_N$ gametes (measured as the deviation from the Mendelian expectation of 0.25) in IL-backcrosses is affected by genetic background, cross direction, and identity of the recurrent parent.

Effect[1]	df	*F*	*P*	LSM	
Background[2]	1	8.259	0.045	G: -0.095	N: -0.149
Cross direction[3]	1	30.910	0.005	♂: -0.174	♀: -0.070
Recurrent parent[4]	1	7.359	0.053	G: -0.147	N: -0.097

[1]Effects assessed by ANOVA with degrees of freedom (df), F-ratio (*F*), p-values (*P*), and least squares means (LSM) indicated.
[2]Crosses performed using fourth-generation NILs. *M. nasutus* background = BN_4; *M. guttatus* background = BG_4.
[3]Cross direction indicates whether the NIL was used as the paternal (♂) or maternal (♀) parent.
[4]Testcrosses were to the IM62 line of *M. guttatus* (G) or the SF line of *M. nasutus* (N).

Table S3. Genotype counts for progeny from reciprocal backcrosses between IM62 and the doubly heterozygous IL-N (*hms1*$_{GN}$; *hms2*$_{GN}$).

	hms1; *hms2* genotype			
Maternal parent	GG; GG	GG; GN	GN; GG	GN; GN
IL-N	105	45	105	99
IM62	35	3	31	35